



Asymptotic behavior analysis of a biodenitrification process model

Mostafa Abaali, Salih Ouchtout

► To cite this version:

Mostafa Abaali, Salih Ouchtout. Asymptotic behavior analysis of a biodenitrification process model. 2023. [⟨hal-03745899v2⟩](#)

HAL Id: hal-03745899

<https://hal.science/hal-03745899v2>

Preprint submitted on 5 Apr 2023

HAL is a multi-disciplinary open access archive for the deposit and dissemination of scientific research documents, whether they are published or not. The documents may come from teaching and research institutions in France or abroad, or from public or private research centers.

L'archive ouverte pluridisciplinaire **HAL**, est destinée au dépôt et à la diffusion de documents scientifiques de niveau recherche, publiés ou non, émanant des établissements d'enseignement et de recherche français ou étrangers, des laboratoires publics ou privés.



HAL Authorization

Asymptotic behavior analysis of a biodenitrification process model *

Mostafa Abaali

Engineering Sciences Lab, ESL ENSA, Ibn Tofail University.[†]
mostafaabaali@gmail.com

Salih Ouchtout

Laboratory of EDP, Algebra and Spectral geometry, EIMA, Department of Mathematics.[‡]
salih.ouchtout@uit.ac.ma

Received (Day Mth. Year)

Revised (Day Mth. Year)

Massive and excessive use of nitrogen fertilizers and sustained irrigation have been widely practised in recent years. This strategy leads to a large transfer of nitrates to groundwater, leading to a major environmental problem of nitrate contamination in water, intended for drinking water consumption. One of the most effective solutions is the degradation of nitrites and nitrates, into gaseous nitrogen, using the heterotrophic bacteria during the denitrification process. In this paper, we present and study a mathematical model of the biodenitrification process taking into account the fixed and mobile bacteria. This process is modeled by a system of ordinary differential equations and requires the success of bacteria to colonize the reactor. We study the existence and the asymptotic behaviour of the solution. We show the existence of a value of the injected carbon concentration from which we ensure the success of the biodenitrification process and we propose a heuristic algorithm which serves to control the biodenitrification process over time. Finally, we perform some numerical simulations in agreement with the theoretical results.

Keywords: Bioprocesses; Biodenitrification; Ordinary differential equations; Asymptotic behaviour.

1. Introduction

Food safety and environmental protection are two key issues in nowadays societies. Due to a remarkable increase of the world population and in order to increase the yield of agricultural production, massive and excessive use of nitrogen fertilizers and sustained irrigation have been widely practised in recent years. This strategy leads to a large transfer of nitrates to groundwater, leading to a major environmental problem of nitrate contamination in water, intended for drinking water consumption. However, the natural environment can offer a possibility of remediation. One of

*Asymptotic behavior analysis of a biodenitrification process Model

[†]*Ibn Tofail University B.P 241, 14000 Kenitra, Morocco.*

[‡]*Ibn Tofail University B.P 133, 14000 Kenitra.*

the most effective solutions is the degradation of nitrites and nitrates, into gaseous nitrogen, is the use of heterotrophic bacteria during the denitrification process. This process is characterized by the fact that when the oxygen concentration is negligible, it will be replaced by oxidized nitrogen (NO_2 and/or NO_3) which is the best electron acceptor after oxygen so the biodenitrification process can be described as a respiratory process in which denitrifying bacteria use nitrates instead of oxygen as an acceptor of electrons [12,8,21]. It generally takes place under conditions, called anoxic, intended to provide energy for cell activity and the synthesis of new cells [18,20,14]. Successful biodenitrification process requires that the nitrate should be considered in the modeling as a limiting compound [2]. In [3], the authors studied the dynamics of potassium in the rhizosphere of the wheat root in the presence and in the absence of a biophysical source and they showed that the presence of bio-fertilizer leads to significant changes in potassium concentration in the rhizosphere of the wheat root. In [4], the authors proposed a mathematical model to study the effect of water flux on nitrate dynamics in the rhizosphere of a single maize root taking into account important mechanisms such as diffusion and mass flux of solutes in the rhizosphere. Charpentier et al. [10] modeled the Trichloroethylene (TCE) biodegradation process where they considered two types of bacteria, the first one degrades the contaminant while the second forms a biobarrier to prevents the contamination from infiltration into groundwater. They gave four spatialized models according to the consumption of the nutrient by the two types of bacteria. In [11] Charpentier et al. gave numerical simulations of several types of collaboration of two types of bacteria to control pollutants are given. Recent theoretical and experimental studies on biofilms [9,13,19] confirm that the growth of bacteria on the walls can be a serious problem for bioreactors and fermenters and have fundamental implications for natural environments. But in biodegradation processes, colonization of the reactor by bacteria can be useful for the results obtained. Freter et al. [15,16] confirmed that adherent bacteria play an important role in the observed stability of the microflora of the mammalian large intestine to colonization by invading organisms. For biodegradation processes, adherent bacteria also play an important role for the evolution of bacteria in the reactor because free bacteria can be influenced by the flow rate. F. Chevron [12], during the experiments, has confirmed the existence of free bacteria in the reactors which accelerated the biodenitrification. M. Ballyk et al. [5] analyzed the case of a single strain of bacteria for the general model given by Ballyk et al. [6] they have shown that there are two possible steady state regimes, the first is the total leaching of bacteria from the reactor(washout) and the second is the successful colonization of the reactor by the bacterial strain. They have shown that one of these regimes is stable under conditions related to system parameters. The main objective of the present paper is to give deeper insights and predictions on the evolution of bacteria and substrates involved in the biodenitrification process with the help of a mathematical model, and consequently their exploitation in heuristic and/or optimal control algorithms.

The paper is organized as follows. In the next section, model and assumptions

are presented and discussed. Then, the dynamics is mathematically analyzed in the following section. In particular, we show that there exists a value of the injected carbon concentration from which we ensure the success of the biodenitrification process. Finally, we perform some numerical simulations in agreement with the theoretical results and we propose a heuristic algorithm to control the biodenitrification process.

2. Mathematical model

In order to describe the mathematical model that governs the water biodenitrification process, we consider that the reactor contains nitrified water, denitrifying bacteria and nutrients. The bacteria in the reactor are divided into two categories: a first type which adhere to the walls of the reactor with a maximum value denoted by ω_∞ , forming a biofilm, denoted by b_f , and a second type which remain mobile and free floating, called planktonic cells and denoted by b_m . The evolution of each type of bacteria is given by the following equation (see [1])

$$\frac{db_i}{dt} = \left(\mu_i(S) - K_i \right) b_i, \quad \text{for } i = m, f, \quad (2.1)$$

where $b_i(t)$ and $S(t)$ represent respectively the concentrations of bacteria and substrate at time t . Symbols K_i and μ_i are successively the loss coefficient (mortality, change of category, ...) and the specific growth rate which will be described later. These denitrifying bacteria react with the contaminant nitrate, considered as an electron acceptor, its concentration will be denoted by S_N . Moreover, bacteria also need carbon for its growth, its concentration will be denoted by S . The input substrate concentrations of S and S_N are respectively S^{in} and S_N^{in} , and we consider that denitrified water is extracted at the outlet of the reactor. Based on the fundamental relations of biological kinetic (that are the growth rate of bacteria and the use rate of the substrate), the evolution of the concentrations S and S_N , is governed respectively by the following equations [1]

$$\frac{dS}{dt} = (S^{in} - S)d_S - \frac{1}{Y_m}b_m\mu_m(\cdot) - \frac{1}{Y_f}\gamma^{-1}b_f\mu_f(\cdot), \quad (2.2)$$

$$\frac{dS_N}{dt} = (S_N^{in} - S_N)d_{S_N} - \frac{R}{Y_m}b_m\mu_m(\cdot) - \frac{R}{Y_f}\gamma^{-1}b_f\mu_f(\cdot), \quad (2.3)$$

where Y_m and Y_f are successively the yield coefficient of mobile bacteria adherent bacteria. Parameters R , d_S and d_{S_N} represent respectively the degradation rate of nitrates, the substrate dilution rate and the nitrate dilution rate. Symbol γ represents the conversion coefficient from volume density to areal density. It can be considered as the ratio between the surface and the perimeter of a section of the domain in the flow direction [5].

Generally, the evolution of the bacteria b_f and b_m depend on each other. In what follow, we describe and introduce this interdependence.

- We take firstly the equation (2.1) governing the fixed bacteria i.e. "i=f", and we consider that the loss coefficient K_f is the sum of both the mortality rate, denoted k_f , and the term corresponding to the detachment rate of these bacteria from surfaces, denoted by β , then we have

$$K_f = k_f + \beta, \quad (2.4)$$

In agreement with [15] and [16], only a proportion of the daughter cells of the fixed bacteria find place on the surface of the reactor, the rest of cells will be evacuated into the liquid. Let us consider the variable \bar{b}_f defined by

$$\bar{b}_f := \frac{b_f}{\omega_\infty}. \quad (2.5)$$

The first proportion of daughter cells is a function of \bar{b}_f (see [15]), denoted by $G(\bar{b}_f)$. In what follows we use the Freter's formula (see [16]), given by

$$G(X) = \frac{1 - X}{a + 1 - X}, \quad (2.6)$$

where a is a very small constant. Therefore, the growth rate of the fixed bacteria in the evolution equation (2.1) will be multiplied by the proportion $G(\bar{b}_f)$. Taking into account these improvements, from (2.1)-(2.6)-(2.4) we get

$$\frac{db_f}{dt} = \left(\mu_f(\cdot)G(\bar{b}_f) - k_f - \beta \right) b_f. \quad (2.7)$$

In addition, a portion of planktonic bacteria can be attached to surfaces with a rate α . Therefore, the term αb_m will be added to the equation (2.7) as source term. We consider $(1 - \bar{b}_f)$ as the availability of the adhesion surface and we introduce γ the conversion coefficient of the volume density into a surface density. Taking into account these progress, the equation (2.7) becomes

$$\frac{db_f}{dt} = \left(\mu_f(\cdot)G(\bar{b}_f) - k_f - \beta \right) b_f + \alpha(1 - \bar{b}_f)\gamma b_m. \quad (2.8)$$

- Moving to the mobile bacteria, similarly to the previous case, we consider that the loss coefficient K_m is the sum of both the mortality coefficient, denoted by k_m , the dilution coefficient denoted by d and the attachment coefficient of mobile bacteria denoted by α i.e. $K_m = k_m + \alpha + d$. The evolution equation (2.1) of b_m becomes

$$\frac{db_m}{dt} = \left(\mu_m(\cdot) - k_m - \alpha - d \right) b_m.$$

In addition, the following modelling improvements will be introduced to this equation. The source term corresponding to the surface concentration of the detached fixed bacteria, multiplied by the conversion coefficient, will

be considered and denoted by $\gamma^{-1}\beta b_f$. The concentration of bacteria which do not find a location to attach themselves will be taken into account and denoted by the term: $b_f\gamma^{-1}\mu_f(\cdot)(1 - G(\bar{b}_f))$. We obtain

$$\frac{db_m}{dt} = \left(\mu_m(\cdot) - k_m - \alpha - d \right) b_m + \gamma^{-1} b_f \left(\mu_f(\cdot)(1 - G(\bar{b}_f)) + \beta \right). \quad (2.9)$$

Finally, from the equations (2.8), (2.9), (2.2) and (2.3), we obtain the following system (2.10) describing the evolution of the quantities (b_f, b_m, S, S_N) of the biodenitrification model.

$$\begin{cases} \frac{db_f}{dt} = \left(\mu_f(\cdot)G(\bar{b}_f) - k_f - \beta \right) b_f + \alpha\gamma(1 - \bar{b}_f)b_m, \\ \frac{db_m}{dt} = \left(\mu_m(\cdot) - k_m - d - \alpha(1 - \bar{b}_f) \right) b_m + \left(\mu_f(\cdot)(1 - G(\bar{b}_f)) + \beta \right) \gamma^{-1} b_f, \\ \frac{dS}{dt} = (S^{in} - S)d_S - \left(\frac{\mu_m(\cdot)}{Y_m} \right) b_m - \left(\frac{\mu_f(\cdot)}{Y_f} \gamma^{-1} \right) b_f, \\ \frac{dS_N}{dt} = (S_N^{in} - S_N)d_{S_N} - \left(\frac{R\mu_m(\cdot)}{Y_m} \right) b_m - \left(\frac{R\mu_f(\cdot)}{Y_f} \gamma^{-1} \right) b_f. \end{cases} \quad (2.10)$$

At time $t = 0$, we assume that the reactor contains nitrified water with an initial density S_N^0 , mobile bacteria with an initial density b_m^0 , fixed bacteria with an initial density b_f^0 and substrate with an initial density S^0 .

$$\begin{cases} b_f(0) = b_f^0, \\ b_m(0) = b_m^0, \\ S(0) = S^0, \\ S_N(0) = S_N^0. \end{cases} \quad (2.11)$$

It is natural to assume that the initial quantities of the variables are positive

$$b_f^0 \geq 0, \quad b_m^0 \geq 0, \quad S \geq 0, \quad S_N \geq 0.$$

In what follows, we will study the existence, characteristics, asymptotic behaviour of the solution and stability of the steady states for the non-spatialized system (2.10), where we assume that the concentrations are uniformly distributed over the whole domain, given by [2] for the purpose of generalizing the results to the spacialized problem.

In order to simplify the presentation of the system, we consider the following notations

$$b_f = c_1, \quad b_m = c_2, \quad S = c_3, \quad S_N = c_4 \quad \text{and} \quad \mathbf{C} = (c_1, c_2, c_3, c_4).$$

6 Mostafa Abaali and Salih Ouchtout

The system (2.10) becomes:

$$\begin{cases} \frac{dc_1}{dt} = F_1(t, \mathbf{C}), \\ \frac{dc_2}{dt} = F_2(t, \mathbf{C}), \\ \frac{dc_3}{dt} = F_3(t, \mathbf{C}), \\ \frac{dc_4}{dt} = F_4(t, \mathbf{C}), \end{cases} \quad (2.12)$$

where

$$\begin{cases} F_1(t, \mathbf{C}) = \left(\mu_f(c_3(t), c_4(t))G\left(\frac{c_1}{\omega_\infty}(t)\right) - k_f - \beta \right) c_1(t) + \alpha\gamma\left(1 - \frac{c_1}{\omega_\infty}(t)\right)c_2(t), \\ F_2(t, \mathbf{C}) = \left(\mu_m(c_3(t), c_4(t)) - k_m - d - \alpha\left(1 - \frac{c_1}{\omega_\infty}(t)\right) \right) c_2(t) \\ \quad + \left(\mu_f(c_3(t), c_4(t))(1 - G\left(\frac{c_1}{\omega_\infty}(t)\right)) + \beta \right) \gamma^{-1} c_1(t), \\ F_3(t, \mathbf{C}) = (c_3^{in} - c_3)d_S - \left(\frac{\mu_m(c_3(t), c_4(t))}{Y_m} \right) c_2(t) - \left(\frac{\mu_f(c_3(t), c_4(t))}{Y_f} \gamma^{-1} \right) c_1(t), \\ F_4(t, \mathbf{C}) = (c_4^{in} - c_4)d_{S_N} - \left(\frac{R\mu_m(c_3(t), c_4(t))}{Y_m} \right) c_2(t) - \left(\frac{R\mu_f(c_3(t), c_4(t))}{Y_f} \gamma^{-1} \right) c_1(t), \end{cases} \quad (2.13)$$

and

$$\begin{cases} c_1(0) = c_1^0 > 0, \\ c_2(0) = c_2^0 > 0, \\ c_3(0) = c_3^0 > 0, \\ c_4(0) = c_4^0 > 0. \end{cases} \quad (2.14)$$

As we have mentioned before, μ_f and μ_m represent the growth function of adherent and free bacteria, respectively, and can obey the multiplicative formula (see [2])

$$\mu_i(c_3, c_4) = \mu_{max}^i \left(\frac{c_3}{c_3 + K_1^i} \right) \left(\frac{c_4}{c_4 + K_2^i} \right), \quad i = f, m \quad (2.15)$$

where the indices $i = m$ and $i = f$ designate respectively free and adherent bacteria. μ_{max}^i is maximum growth rate. The constants K_j^i , for $i = m, f$ and $j = 1, 2$, ("j = 1" relates to consumption of nutrient and "j = 2" relates to consumption of nitrates) are in fact the Monod's law constants, also called the half-saturation constants. (see the profile of μ_i in Figure 1, for example for $\mu_{max}^i = 0.7$, $K_1^i = 60$ and $K_2^i = 50$).

According to [2], the functions G and $\mu_i(\cdot, \cdot)$ satisfy the following properties.
hypothesis

H1) The specific growth rate function of bacteria $\mu_i(x, y)$, for $i = f, m$, satisfies

$$\mu_i \in C^1, \quad \mu_i(0, y) = \mu_i(x, 0) = 0.$$

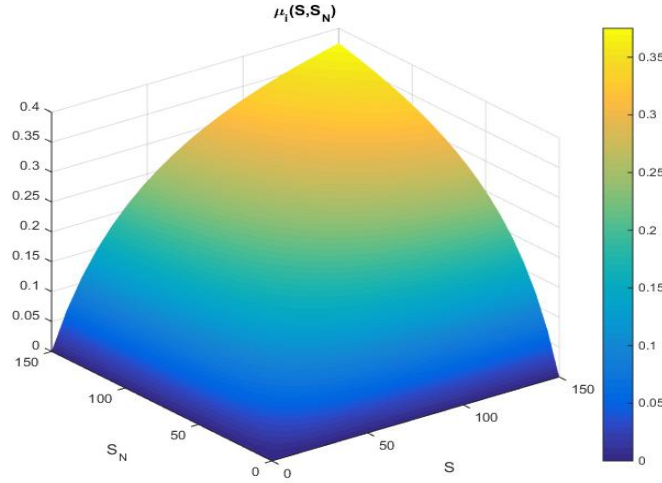


Figure 1: Graphs of multiplicative function μ_i , $i = f, m$ with $\mu_{max}^i = 0.7$, $K_1^i = 60$ and $K_2^i = 50$.

H2) The function G is bounded such that

$$G \in C^1, \quad 0 < G(0) \leq 1, \quad G(1) = 0.$$

3. Asymptotic behaviour study

Definition 3.1. The function \mathcal{F} such that $\mathcal{F} := (\mathcal{F}_1, \mathcal{F}_2, \dots, \mathcal{F}_p) \in C^1(\mathbb{R}_+ \times \mathbb{R}^p, \mathbb{R}^p)$ with $p \in \mathbb{N}^*$ is quasi-positive if

$$\mathcal{F}_i(t, y) \geq 0 \quad \text{whenever} \quad (t, y) \in (0, +\infty) \times \mathbb{R}_+^p \quad \text{is such that} \quad y_i = 0.$$

Proposition 3.2. Under Hypothesis 2.1 the system (2.13) admits a nonnegative maximal solution.

Proof. The functions F_i for $i = 1, 2, 3, 4$ are Lipschitz and then according to the Cauchy-Lipschitz theorem, the system (2.13) admits a maximal solution. In addition, the function $F = (F_1, F_2, F_3, F_4)$ is quasi-positive and consequently the solutions are nonnegative (see [7] page 3). \square

Proposition 3.3. Let (c_1, c_2, c_3, c_4) be the solution of (2.13), where $c_i^0 \leq c_i^{in}$ for $i = 3, 4$. We consider the following quantities

$$M_1 = \max \left(\mu_f(c_3^{in}, c_4^{in}) - k_f; \mu_m(c_3^{in}, c_4^{in}) - k_m - d \right),$$

$$M_2 = \min \left(\mu_f(c_3, c_4) - k_f; \mu_m(c_3, c_4) - k_m - d \right).$$

Thus,

- if $M_1 \leq 0$, then $\gamma^{-1}c_1(t) + c_2(t) \leq \gamma^{-1}c_1^0 + c_2^0$.
- if $M_2 \geq 0$, then $\gamma^{-1}c_1(t) + c_2(t) \geq \gamma^{-1}c_1^0 + c_2^0$.

Proof.

Multiplying the first equation of the system (2.13) by γ^{-1} and then making the sum of the first and the second equation of the system (2.13), we get

$$\frac{d(\gamma^{-1}c_1 + c_2)}{dt} = \gamma^{-1}(\mu_f(c_3, c_4) - k_f)c_1 + (\mu_m(c_3, c_4) - k_m - d)c_2.$$

Or the functions μ_f and μ_m are increasing, for each variable, so

$$M_2(\gamma^{-1}c_1 + c_2) \leq \frac{d(\gamma^{-1}c_1 + c_2)}{dt} \leq M_1(\gamma^{-1}c_1 + c_2).$$

If $M_1 \leq 0$ then the function $(\gamma^{-1}c_1 + c_2)(t)$ decrease from where

$$\forall t \geq t_0, (\gamma^{-1}c_1 + c_2)(t) \leq \gamma^{-1}c_1^0 + c_2^0.$$

If $M_2 \geq 0$ then the function $(\gamma^{-1}c_1 + c_2)(t)$ increase from where

$$\forall t \geq t_0, (\gamma^{-1}c_1 + c_2)(t) \geq \gamma^{-1}c_1^0 + c_2^0. \quad \square$$

Remark 3.4.

- The first point of Theorem 3.3 confirms that the concentration of bacteria will be lower than the initial data and therefore the bacteria will die out and the biodegradation process will be unsuccessful.
- The second point of Theorem 3.3 confirms that the concentration of bacteria will be greater than the initial data, and consequently the bacteria will succeed in colonizing the reactor and the biodegradation process will be successful.

Corollary 3.5. *Let (c_1, c_2, c_3, c_4) be the solution of (2.13). Under the Hypothesis 2.1, for $i = 3$ or 4 , we get*

$$c_i(t) \leq c_i^{in} \quad \forall t > 0.$$

Proof. Thanks to Theorem 3.2, for $i = 1$ or 2 we have $c_i \geq 0$ then

$$\begin{cases} \frac{dc_3}{dt} \leq (c_3^{in} - c_3)d_S, \\ \frac{dc_4}{dt} \leq (c_4^{in} - c_4)d_{S_N}, \end{cases}$$

which implies

$$\begin{cases} \frac{d(c_3 - c_3^{in})}{dt} \leq -(c_3 - c_3^{in})d_S, \\ \frac{d(c_4 - c_4^{in})}{dt} \leq -(c_4 - c_4^{in})d_{S_N}, \end{cases}$$

equivalent to

$$\begin{cases} \frac{d(c_3 - c_3^{in})}{dt} \leq (c_3 - c_3^{in})(-d_S), \\ \frac{d(c_4 - c_4^{in})}{dt} \leq (c_4 - c_4^{in})(-d_{S_N}). \end{cases}$$

By using the Gronwall's lemma we get

$$\begin{cases} c_3 - c_3^{in} \leq (c_3^0 - c_3^{in}) \exp(-d_S t), \\ c_4 - c_4^{in} \leq (c_4^0 - c_4^{in}) \exp(-d_{S_N} t), \end{cases}$$

and by the fact that $c_3^0 \leq c_3^{in}$ and $c_4^0 \leq c_4^{in}$ we obtain

$$\begin{cases} c_3 - c_3^{in} \leq 0, \\ c_4 - c_4^{in} \leq 0, \end{cases}$$

Finally we get

$$\begin{cases} c_3 \leq c_3^{in}, \\ c_4 \leq c_4^{in}. \end{cases} \quad \square$$

Proposition 3.6. *There exists a value c_3^* such that for any c_3^{in} verifying the inequality $c_3^{in} < c_3^*$ we get $M_1 < 0$, where*

$$c_3^* = \min \left(\frac{(K_2^f + c_4^{in})k_f(K_1^f + \mu_{max}^f)}{c_4^{in}\mu_{max}^f}, \frac{(K_2^m + c_4^{in})(k_m + d)(K_1^m + \mu_{max}^m)}{c_4^{in}\mu_{max}^m} \right). \quad (3.1)$$

Proof. .

The conditions for that $M_1 < 0$ are

$$\mu_f(c_3^{in}, c_4^{in}) - k_f < 0, \quad (3.2)$$

and

$$\mu_m(c_3^{in}, c_4^{in}) - k_m - d < 0. \quad (3.3)$$

According to (2.15), the first condition eq. (3.2) implies

$$\begin{aligned} & \mu_{max}^f \frac{c_3^{in}}{K_1^f + c_3^{in}} \times \frac{c_4^{in}}{K_2^f + c_4^{in}} - k_f < 0 \\ \Leftrightarrow & \frac{c_3^{in}}{K_1^f + \mu_{max}^f} < \frac{(K_2^f + c_4^{in})k_f}{c_4^{in}\mu_{max}^f} \\ \Leftrightarrow & c_3^{in} < \frac{(K_2^f + c_4^{in})k_f(K_1^f + \mu_{max}^f)}{c_4^{in}\mu_{max}^f}. \end{aligned} \quad (3.4)$$

The second condition eq. (3.3) implies

$$\begin{aligned}
& \mu_{max}^m \frac{c_3^{in}}{K_1^m + c_3^{in}} \times \frac{c_4^{in}}{K_2^m + c_4^{in}} - k_m - d < 0 \\
& \Leftrightarrow \frac{c_3^{in}}{K_1^m + \mu_{max}^m} < \frac{(K_2^m + c_4^{in})(k_m + d)}{c_4^{in} \mu_{max}^m} \\
& \Leftrightarrow c_3^{in} < \frac{(K_2^m + c_4^{in})(k_m + d)(K_1^m + \mu_{max}^m)}{c_4^{in} \mu_{max}^m} \quad (3.5)
\end{aligned}$$

From (3.4) and (3.5), we obtain

$$c_3^{in} < \min\left(\frac{(K_2^f + c_4^{in})k_f(K_1^f + \mu_{max}^f)}{c_4^{in} \mu_{max}^f}, \frac{(K_2^m + c_4^{in})(k_m + d)(K_1^m + \mu_{max}^m)}{c_4^{in} \mu_{max}^m}\right) = c_3^*. \square$$

Proposition 3.7. *Let (c_1, c_2, c_3, c_4) be the solution of (2.13). The following properties hold true:*

- If $M_1 < 0$, then $\lim_{t \rightarrow \infty} (\gamma^{-1}c_1(t) + c_2(t)) = 0$.
- If $M_2 > 0$, then $\lim_{t \rightarrow \infty} (\gamma^{-1}c_1(t) + c_2(t)) = c^* > \gamma^{-1}c_1^0 + c_2^0$.
- $\lim_{t \rightarrow \infty} c_3(t) \leq c_3^{in}$.
- $\lim_{t \rightarrow \infty} c_4(t) \leq c_4^{in}$.

Proof.

- By multiplying the first equation of (2.12) by γ^{-1} and making the sum of the first and the second equation of the system (2.12), we get

$$\frac{d(\gamma^{-1}c_1 + c_2)}{dt} = \gamma^{-1} \left(\mu_f(c_3, c_4) - k_f \right) c_1 + \left(\mu_m(c_3, c_4) - k_m - d \right) c_2$$

which implies

$$M_2 \left(\gamma^{-1}c_1 + c_2 \right) \leq \frac{d(\gamma^{-1}c_1 + c_2)}{dt} \leq M_1 \left(\gamma^{-1}c_1 + c_2 \right).$$

By using the Gronwall's lemma we have $0 \leq (\gamma^{-1}c_1 + c_2) \leq (\gamma^{-1}c_1^0 + c_2^0)e^{M_1 t}$ since $M_1 < 0$ and for $t \rightarrow \infty$ then we obtain the result.

- For the adherent bacteria and from eq. (2.5), we have $c_1 \leq \omega_\infty$. For the free bacteria and according to the growth function proprieties there exists a maximal concentration c_2^{max} such that $c_2 \leq c_2^{max}$, which gives

$$\gamma^{-1}c_1(t) + c_2(t) \leq \gamma^{-1}\omega_\infty + c_2^{max}.$$

Or $M_2 > 0$, then the concentration $(\gamma^{-1}c_1 + c_2)$ is increasing, respecting time, and bounded. Then there exists a value c^* such that

$$\lim_{t \rightarrow \infty} (\gamma^{-1}c_1(t) + c_2(t)) = c^* > \gamma^{-1}c_1^0 + c_2^0.$$

- According to Theorem 3.2, we have $c_i \geq 0$, $i = 1, 2$ then

$$\begin{cases} \frac{dc_3}{dt} \leq (c_3^{in} - c_3)d_S, \\ \frac{dc_4}{dt} \leq (c_4^{in} - c_4)d_{S_N}, \end{cases} \quad (3.6)$$

which implies

$$\begin{cases} \frac{d(c_3 - c_3^{in})}{dt} \leq -(c_3 - c_3^{in})d_S, \\ \frac{d(c_4 - c_4^{in})}{dt} \leq -(c_4 - c_4^{in})d_{S_N}, \end{cases} \quad (3.7)$$

equivalent to

$$\begin{cases} \frac{d(c_3 - c_3^{in})}{dt} \leq (c_3 - c_3^{in})(-d_S), \\ \frac{d(c_4 - c_4^{in})}{dt} \leq (c_4 - c_4^{in})(-d_{S_N}). \end{cases} \quad (3.8)$$

Using the Gronwall's lemma, we get

$$\begin{cases} c_3 - c_3^{in} \leq (c_3^0 - c_3^{in}) \exp(-d_S t), \\ c_4 - c_4^{in} \leq (c_4^0 - c_4^{in}) \exp(-d_{S_N} t), \end{cases} \quad (3.9)$$

which implies

$$\begin{cases} c_3 \leq (c_3^0 - c_3^{in}) \exp(-d_S t) + c_3^{in}, \\ c_4 \leq (c_4^0 - c_4^{in}) \exp(-d_{S_N} t) + c_4^{in}. \end{cases} \quad (3.10)$$

Finally we obtain $\lim_{t \rightarrow +\infty} c_3 \leq c_3^{in}$ and $\lim_{t \rightarrow +\infty} c_4 \leq c_4^{in}$ □

In what follows, we study the existence and stability of the steady state.

By combining the first and the second equation of (2.12) in a single equation, the system (2.12) can be writing in the following form

$$\begin{cases} \frac{d(\gamma^{-1}c_1 + c_2)}{dt} = \gamma^{-1} \left(\mu_f(c_3, c_4) - k_f \right) c_1 + \left(\mu_m(c_3, c_4) - k_m - d \right) c_2, \\ \frac{d(c_3)}{dt} = (c_3^{in} - c_3)d_S - \left(\frac{\mu_m(c_3, c_4)}{Y_m} \right) c_2 - \left(\frac{\mu_f(c_3, c_4)}{Y_f} \gamma^{-1} \right) c_1, \\ \frac{d(c_4)}{dt} = (c_4^{in} - c_4)d_{S_N} - \left(\frac{R\mu_m(c_3, c_4)}{Y_m} \right) c_2 - \left(\frac{R\mu_f(c_3, c_4)}{Y_f} \gamma^{-1} \right) c_1. \end{cases} \quad (3.11)$$

We make a change of variable

- $\tilde{c} = \gamma^{-1}c_1 + c_2$,
- $\mu(c_3, c_4)\tilde{c} = \mu_f(c_3, c_4)\gamma^{-1}c_1 + \mu_m(c_3, c_4)c_2$,
- $K\tilde{c} = k_f\gamma^{-1}c_1 + (k_m + d)c_2$,
- $\frac{\mu(c_3, c_4)}{Y}\tilde{c} = \left(\frac{\mu_m(c_3, c_4)}{Y_m} \right) c_2 + \left(\frac{\mu_f(c_3, c_4)}{Y_f} \gamma^{-1} \right) c_1$.

The system (3.11) then can be written as follows with three variables

$$\begin{cases} \frac{d\tilde{c}}{dt} = (\mu(c_3, c_4) - K)\tilde{c}, \\ \frac{dc_3}{dt} = (c_3^{in} - c_3)d_S - \frac{\mu(c_3, c_4)}{Y}\tilde{c}, \\ \frac{dc_4}{dt} = (c_4^{in} - c_4)d_{S_N} - \frac{R\mu(c_3, c_4)}{Y}\tilde{c}. \end{cases} \quad (3.12)$$

The steady states, denoted by $(\tilde{c}^*, c_3^*, c_4^*)$, of the system (3.12) verify

$$\begin{cases} 0 = (\mu(c_3^*, c_4^*) - K)\tilde{c}^*, \\ 0 = (c_3^{in} - c_3^*)d_S - \frac{\mu(c_3^*, c_4^*)}{Y}\tilde{c}^*, \\ 0 = (c_4^{in} - c_4^*)d_{S_N} - \frac{R\mu(c_3^*, c_4^*)}{Y}\tilde{c}^*. \end{cases} \quad (3.13)$$

We remark that the first steady state is the washout steady state and is $(0, c_3^{in}, c_4^{in})$. In addition, the other steady states satisfy

$$\begin{cases} 0 = (c_3^{in} - c_3^*)d_S - \frac{K}{Y}\tilde{c}^*, \\ 0 = (c_4^{in} - c_4^*)d_{S_N} - \frac{RK}{Y}\tilde{c}^*, \end{cases} \quad (3.14)$$

which implies

$$\begin{cases} 0 = (c_3^{in} - c_3^*)d_S - \frac{K}{Y}\tilde{c}^*, \\ c_4^* = \frac{c_4^{in}d_{S_N} - Rd_S(c_3^{in} - c_3^*)}{d_{S_N}}, \end{cases} \quad (3.15)$$

hence

$$\begin{cases} \tilde{c}^* = \frac{Yd_S(c_3^{in} - c_3^*)}{K}, \\ c_4^* = \frac{c_4^{in}d_{S_N} - Rd_S(c_3^{in} - c_3^*)}{d_{S_N}}, \end{cases} \quad (3.16)$$

From the system (3.15), we remark that the system (3.13) admits an infinity of steady states. The linearization of the system (3.13) near the washout steady state is given using the following Jacobian matrix:

$$A = \begin{pmatrix} \mu_f(c_3^{in}, c_4^{in}) - K & 0 & 0 \\ -\frac{\mu_f(c_3^{in}, c_4^{in})}{Y} & -d_S & 0 \\ -\frac{\mu_f(c_3^{in}, c_4^{in})}{Y} & 0 & -d_{S_N} \end{pmatrix},$$

Proposition 3.8. *The following properties hold true.*

- If $M_1 + M_2 < 0$, then the washout steady state is stable.
- If $M_1 + M_2 > 0$, the washout steady state is unstable and there is another state of equilibrium $(\dot{c}_1, \dot{c}_2, \dot{c}_3)$ such that $\dot{c}_1 \geq \gamma^{-1}c_1^0 + c_2^0$ and it is stable.

Proof.

- The condition $M_1 + M_2 < 0$ gives $\mu_f(c_3^{in}, c_4^{in}) - K < 0$ and then the matrix A has three negative eigenvalues and therefore the washout steady state is stable.
- The condition $M_1 + M_2 > 0$ gives $\mu_f(c_3^{in}, c_4^{in}) - K > 0$ and then the matrix A admits a non negative eigenvalue and therefore the washout steady state is unstable. Using the Theorem 3.3 and the fact that the system (3.13) admits a solution then we obtain the result. \square

Numerical algorithm for solving the system:

The functions of the second members of system 2.12 are given in the general form, by writing them as a function of t and of the unknown vector $\mathbf{C}(t) = (c_1(t), c_2(t), c_3(t), c_4(t))$. However, in our case, the system can be written as an autonomous system, i.e. F_i are only functions of $\mathbf{C}(t)$.

The numerical scheme for solving the problem (2.12) has been implemented in Python computational software through the fourth-order Runge-Kutta method (see Algorithm 1). It is an efficient method for solving problems of ordinary differential equations with initial values and it guarantees a stable computing time [17].

Algorithm 1 Numerical algorithm based on RK4 for solving the problem.

```

1: Initialisation:  $t_0$  (initial time),
2:                    $t_f$  (final time),
3:                    $\Delta t$  (the step size),
4:                    $\mathbf{C} \leftarrow \mathbf{C}(t_0)$  (initial conditions).
5: define  $F_i(\mathbf{C})$ ,  $i = 1, 2, 3, 4$ 
6:  $N \leftarrow \frac{t_f - t_0}{\Delta t} + 1$ 
7:  $t \leftarrow t_0$ 
8: for  $k \leftarrow 1$  to  $N$  do
9:    $K_1^i \leftarrow \Delta t F_i(\mathbf{C}(t))$ ,  $i = 1, 2, 3, 4$ 
10:   $K_2^i \leftarrow \Delta t F_i\left(\mathbf{C}(t) + \frac{\Delta t}{2} K_1^i\right)$ ,  $i = 1, 2, 3, 4$ 
11:   $K_3^i \leftarrow \Delta t F_i\left(\mathbf{C}(t) + \frac{\Delta t K_2^i}{2}\right)$ ,  $i = 1, 2, 3, 4$ 
12:   $K_4^i \leftarrow \Delta t F_i(\mathbf{C}(t) + \Delta t K_3^i)$ ,  $i = 1, 2, 3, 4$ 
13:   $c_i(t) \leftarrow c_i(t) + \frac{1}{6}(K_1^i + 2 K_2^i + 2 K_3^i + K_4^i)$ ,  $i = 1, 2, 3, 4$ 
14:  Registration.
15:   $t \leftarrow t + \Delta t$ 
16: end for

```

4. Numerical results

In this section we present some numerical results about the success of the biodenitrification process in agreement with the theoretical results the problem (2.13). The different parameters used are given in Table 2 and come from [2]. From the same reference, we take the initial conditions of the system as indicated in Table 1.

In the theoretical study, we showed the existence of a value c_3^* of the injected carbon concentration from which we ensure the success of the biodenitrification process and the stability of the steady states. To verify that numerically, we perform two numerical experiences. Before that we start to compute the value of c_3^* . For example, with the parameter values given in the Table 2 and according to eq. (3.1), we get $c_3^* = 0.6504mg/l$.

In the first test, we take a value of the amount of carbon injected c_3^{in} such that $c_3^{in} \geq c_3^*$. For example with $c_3^{in} = c_3(0) = 104mg/l$, we get Figure 2, Figure 3 and Figure 4 (evolution/behaviour of bacteria and substrates). Figure 2 shows the evolution of c_1 , c_2 , c_3 and c_4 . Figure 3 shows the evolution of \tilde{c} , c_3 and c_4 and then the stability of the system in agreement with Theorem 3.8. Figure 4 shows the evolution $(\gamma^{-1})c_1 + c_2$ and $(\gamma^{-1})c_1^0 + c_2^0$. We remark in this figure that for $c_3^{in} \geq c_3^*$, bacteria evolve in the reactor and then the success of the biodenitrification process which is consistent with the results obtained in the Theorem 3.3 and the Theorem 3.5. We also observe that from a certain time the four components stagnate which means that we obtain a stable steady state as is confirmed in the Theorem 3.7 and Theorem 3.8.

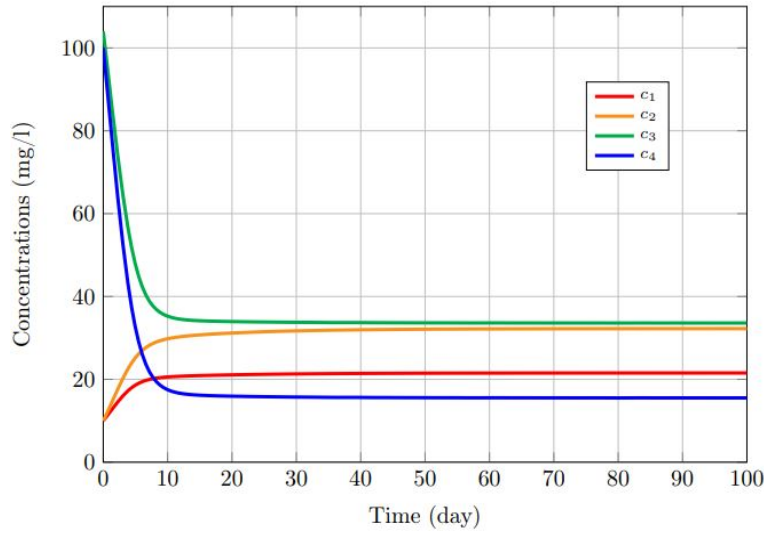
In the second test, we take a value of the amount of carbon injected c_3^{in} such that $c_3^{in} \leq c_3^*$. For example with $c_3^{in} = c_3(0) = 0.5mg/l$, we get Figure 6, Figure 5, and Figure 7. Figure 5 shows the evolution of c_1 , c_2 , c_3 and c_4 . Figure 6 shows the evolution of \tilde{c} , c_3 and c_4 and then the stability of the system in agreement with Theorem 3.8. Figure 7 shows the evolution $(\gamma^{-1})c_1 + c_2$ and $(\gamma^{-1})c_1^0 + c_2^0$. We remark in this figure that for $c_3^{in} \leq c_3^*$, bacteria disappear from the reactor and then the biodenitrification process fails which is consistent with the results obtained in the Theorem 3.3 and the Theorem 3.5, we note that in this case we have $M_1 = -0.0011$, the value given in the Theorem 3.3. We also observe that from a certain time bacteria concentration decreases towards 0 and the concentrations of carbon and nitrates respectively increase towards c_3^{in} and c_4^{in} which means that $(0, 0, c_3^{in}, c_4^{in})$ is a stable steady state as is confirmed in the Theorem 3.7 and Theorem 3.8.

$b_f(t=0)$ (mg/l)	$b_m(t=0)$ (mg/l)	$S_N(t=0)$ (mg/l)	S_N^{in} (mg/l)
10	10	100	100

Table 1: Initial conditions.

Parameters	Values	Parameters	Values
d	$0.1\text{cm}^2/h$	μ_{max}^f	$0.7h^{-1}$
d_{SN}	$0.1\text{cm}^2/h$	Y_m	0.5
d_S	$0.1\text{cm}^2/h$	Y_f	0.5
a	0.1	β	$0.2h^{-1}$
α	$0.2h^{-1}$	T	60 days
w_∞	$60g/cm^2$	R	1.2
γ	$0.8ml/cm^2$	K_1^f	60 mg carbon/l
k_m	$0.005h^{-1}$	K_1^m	60 mg carbon/l
k_f	$0.005h^{-1}$	K_2^m	50 mg NO_3^- /l
μ_{max}^m	$0.7h^{-1}$	K_2^f	50 mg NO_3^- /l

Table 2: Parameters.

Figure 2: Evolution of c_1 , c_2 , c_3 and c_4 with $c_3^{in} = 104 \geq c_3^*$.*Heuristic algorithm for improving the process:*

In the theoretical study of the problem as well as in the previous numerical tests, we showed the existence of a specific value of the injected carbon concentration from which we ensure the success of the biodenitrification process. In this part of numerical results, we propose a heuristic algorithm, based on previous results, to improve and control the biodenitrification process over time.

In what follow, we will present and compare 2 different schemes, to manage

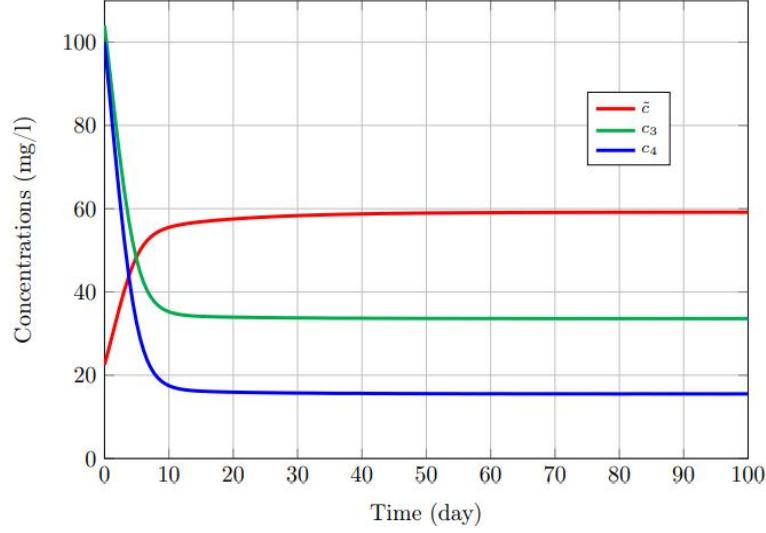


Figure 3: Evolution of \tilde{c} , c_3 and c_4 with $c_3^{in} = 104 \geq c_3^*$.

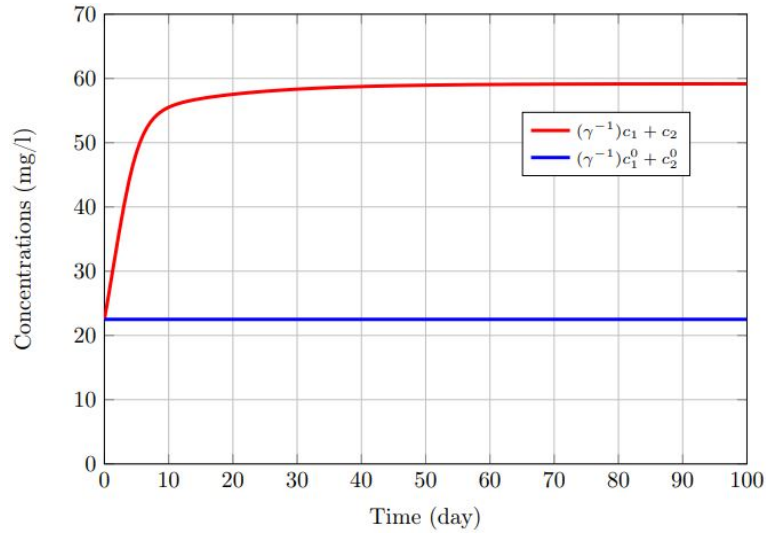


Figure 4: Graphs of bacteria rate $[(\gamma^{-1})c_1 + c_2]$ and initial bacteria rate $[(\gamma^{-1})c_1^0 + c_2^0]$ with $c_3^{in} = 104 \geq c_3^*$.

a total available quantity of c_3 , to improve the process (one of them using our proposed heuristic algorithm Algo. 2). We recall that c_3 is the nutrient that helps bacteria c_2 to increase, and thus the consumption of nitracts c_4 (contamination).

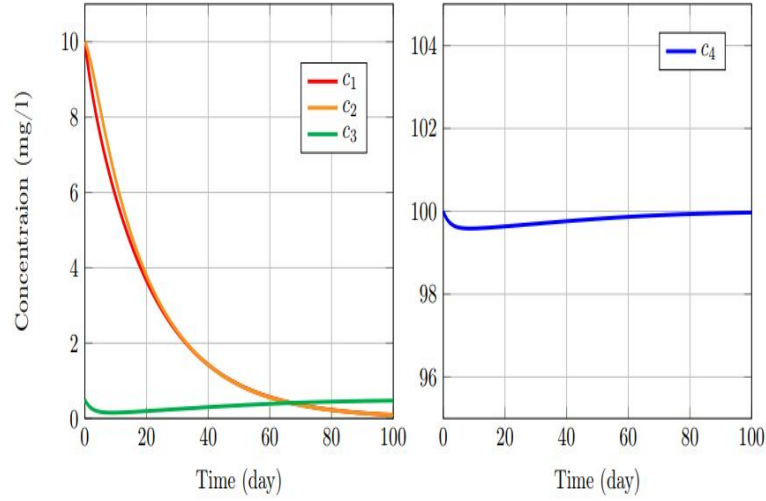


Figure 5: Evolution of c_1 , c_2 , c_3 and c_4 with $c_3^{in} = 0.5 < c_3^*$.

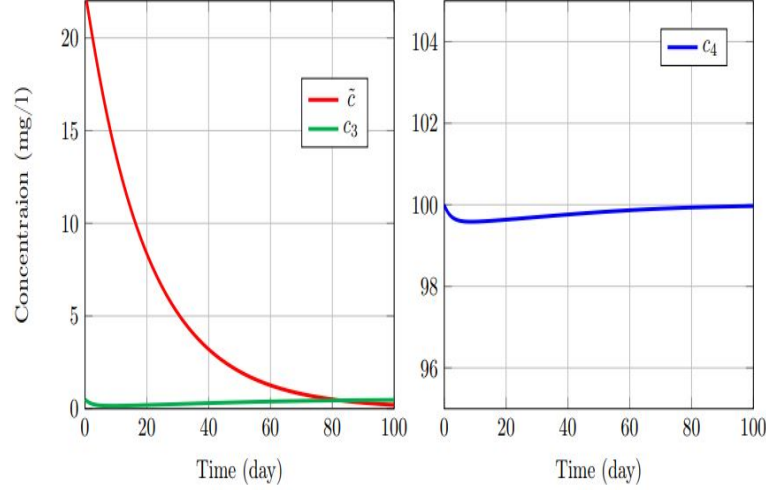


Figure 6: Evolution of \tilde{c} , c_3 and c_4 with $c_3^{in} = 0.5 < c_3^*$.

In both schemes, as already shown, we consider the correct given path that gives the success of the biodenitrification process, ie $c_3^{in} \geq c_3^*$, but in the heuristic algorithm scheme we make several injections of c_3^i until the disappearance of the total available quantity of c_3 to manage, or until the elimination of c_4 (i.e. con-

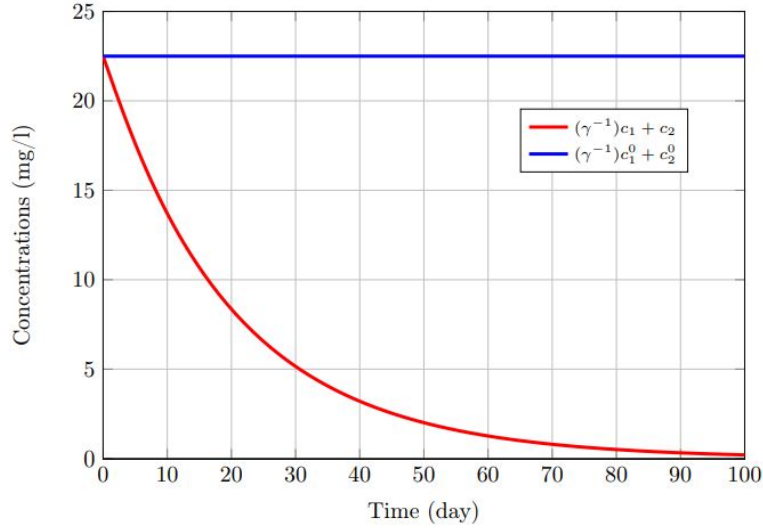


Figure 7: Graphs of bacteria rate $[(\gamma^{-1})c_1 + c_2]$ and initial bacteria rate $[(\gamma^{-1})c_1^0 + c_2^0]$ with $c_3^{in} = 0.5 < c_3^*$.

tamination). Improving biodenitrification involves reducing c_4 as much as possible. As we have shown, this is related to the value of c_3 available in the biodegradable medium. We assume that the total available quantity to manage is denoted by $c_3^{total} := c_3(0) + c_3^{in} + \sum_i c_3^{added,i}$, where $c_3^{added,i}$, $i = 1, 2, \dots$ are the quantities that will be added during different injections over time. In this experiment, we consider for example that $k_f = 0.05$ and $c_4^{in} = 50$ in order to have another value of c_3^* larger than the one we obtained previously. So in this case, we get $c_3^* = 8.6714$ (see line 6 in Algo. 2). In addition, we assume for example that $c_3^{total} = 21.025$.

As we have shown, c_3^{in} must be greater than c_3^* and $c_3^{(t_0)}$. Therefore, we start our heuristic algorithm by choosing $c_3^{in} = c_3^*$ (see line 8 in Algo.2). Then, we solve the system until the equilibrium or when c_4 begins to grow. The stopping time of this resolution is denoted t^* (see line 10 in Algo. 2). At this moment, we inject a quantity, denoted $c_3^{added,1}$ such that we obtain $c_3(t_1) + c_3^{in} = 2c^*$ (see line 13 in Algo. 2). The same step will be done until the consumption of the total available quantity of c_3 to manage (or when $c_4 = 0$).

Figure 8 and Figure 9 show the evolution of c_4 in the two schemes respectively, i.e without the use of the heuristic algorithm (scheme 1) and with the use of the heuristic algorithm (scheme 2), with the same total available quantity c_3^{total} . For scheme 1 the resolution was made on $[0, 100]$ and thus Figure 8 shows the evolution of c_4 on $[0, 100]$, devised over two intervals in order to subsequently show the compared curves. However, with the heuristic algorithm Algo. 2, 3 steps were performed to manage the total available quantity c_3^{total} (see Figure 9). The first resolution was

performed on $[t_0 = 0, t_1 = 39.9]$, and the quantity $c_3^{added,1} = 2.6212$ was injected (and at t_1 : $c_4(t_1) = 47.7757$). The second resolution was performed on $[t_1, t_2 = 44.4]$, and the quantity $c_3^{added,2} = 0.7933$ was injected (and at t_2 : $c_4(t_2) = 47.6265$). The third resolution was performed on $[t_2, t_3 = 45.8]$, and the quantity $c_3^{added,3} = 0.2677$ was injected (and at t_3 : $c_4(t_3) = 47.6137$). At instant t_3 : all the quantity c_3^{total} is consumed ($c_3(0) = 8.6714$, $c_3^{in} = 8.6714$, $c_3^{added,1} = 2.6212$, $c_3^{added,2} = 0.7933$, $c_3^{added,3} = 0.2677$, and $c_3^{total} := c_3(0) + c_3^{in} + \sum_i c_3^{added,i} = 21.025$).

In terms of comparison: with scheme 1, we obtained at $t = 45.8 = t_3$: $c_4(t_3) = 47.8190 =: v_1$, and then it increases to the value 49.5331 at $t = 100$ (see Figure 8). However with the use of Algo. 2, we obtained $c_4(t_3) = 47.6137 = v_2 < v_1$ and we can also follow our process of decreasing c_4 if the total quantity available c_3^{total} to manage is greater. Moreover, with scheme 2, at time t_3 , we have a quantity c_2 greater than that obtained in scheme 1: $c_2(t_3) = 1.0528$ "scheme 1" Vs $c_2(t_3) = 1.1248$ "scheme 2" (c_2 is the bacteria that helps to reduce nitrates c_4).

Algorithm 2 Heuristic algorithm for improving the process.

- 1: **Input** Parameters.
 - 2: **Initialisation:** $t_0 = 0$ (initial time),
 - 3: $c_1(0), c_2(0), c_3(0), c_4(0),$
 - 4: c_3^{total}, c_4^{in} where $c_3^{total} := c_3(0) + c_3^{in} + \sum_i c_3^{added,i}$
 - 5: // c_3^{total} is the total quantity available to manage.
 - 6: **Calcul** c_3^* by using eq. (3.1) and c_4^{in} .
 - 7: // We suppose that at t_0 : $c_3(0) > c_3^*$
 - 8: $c_3^{in} \leftarrow c_3(0)$ // (or $c_3^{in} \leftarrow c_3^*$ if $c_3(0) = c_3^*$)
 - 9: $t_i \leftarrow t_0$
 - 10: (#) : **Solve** the Sys. (2.10) on $[t_i, t^*]$, where t^* is the first moment to achieve equilibrium or when c_4 begins to grow.
 - 11: $t_1 \leftarrow t^*$
 - 12: $c_3^{added,1} \leftarrow c_3^* - c_3(t_1)$
 - 13: $c_3(t_1) \leftarrow c_3(t_1) + c_3^{added,1}$
 - 14: $t_i \leftarrow t_1$
 - 15: **do** (#).
 - 16: $t_2 \leftarrow t^*$
 - 17: $c_3^{added,2} \leftarrow c_3^* - c_3(t_2)$
 - 18: $c_3(t_2) \leftarrow c_3(t_2) + c_3^{added,2}$
 - 19: $t_i \leftarrow t_2$
 - 20: **do** (#).
 - 21: \vdots
 - 22: until the consumption of the total quantity available of c_3 to manage (or when $c_4 = 0$).
-

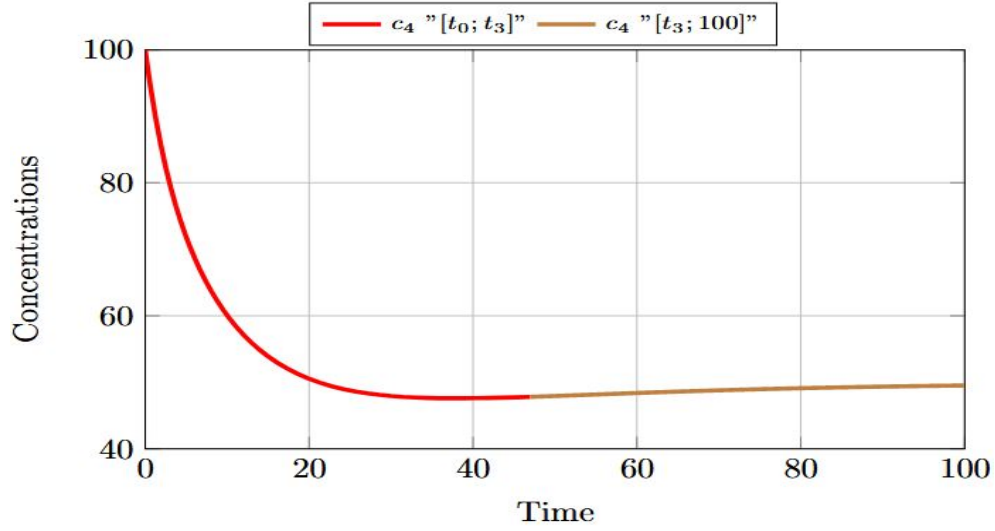


Figure 8: Evolution of c_4 with scheme 1 by solving directly the system on $[0,100]$ (i.e without using the heuristic algorithm). In this plot: $c_4(t_3) = 47.8190$ and $c_4(100) = 49.5331$

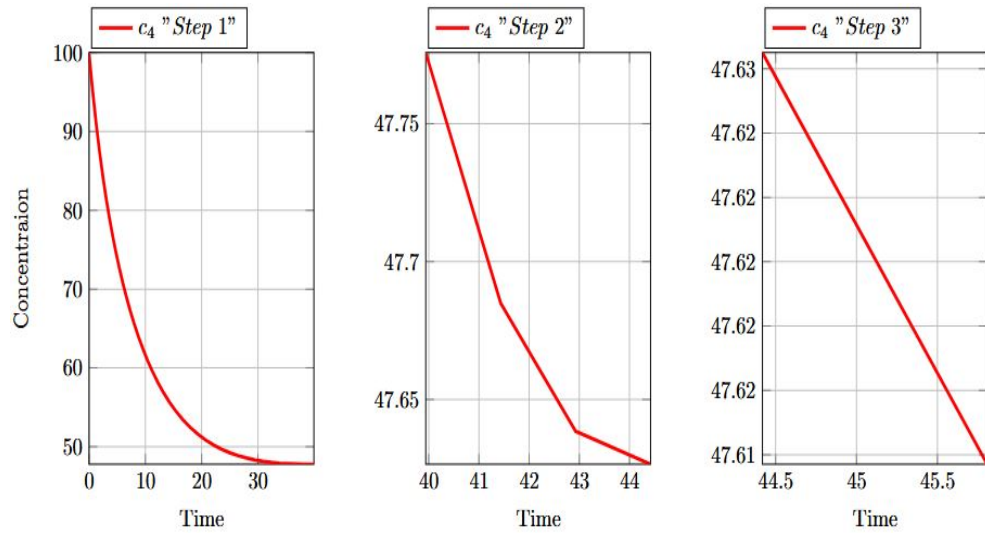


Figure 9: Evolution of c_4 by using our proposed heuristic algorithm Algo. 2 (i.e scheme 2). Step1 is on $[t_0, t_1]$, Step2 is on $[t_1, t_2]$, Step3 is on $[t_2, t_3]$, and at t_3 : $c_4(t_3) = 47.6137$.

5. Conclusion

In this work we have developed a mathematical model dedicated to the biodenitrification process, taking into account the fixed and mobile bacteria. We studied asymptotic behaviour and provided some information for the solution of the problem. The numerical simulations in agreement with the theoretical results show the existence of a value of the injected carbon concentration from which we ensure the success of the biodenitrification process. This study also allowed us to provide a heuristic algorithm in order to improve the situation of biodegradation by minimizing as much as possible the nitrate (contaminant) over time in the environment and then improving the biodenitrification process. As a perspective, taking into account the obtained results, the model can be treated in a complete study of optimal control for choosing optimally the proportion of splitting and the corresponding re-introduction time(s) to obtain the best performances. This could be the matter of a future work. Moreover, the introduction of spatial heterogeneity in the model, in terms of a system of reaction diffusion "partial differential equations" instead of a system of "ordinary differential equations" would be a reasonable extension of the present work, taking into consideration that spatial heterogeneity is usually observed in real problem.

Bibliography

- [1] M. Abaali and Z. Mghazli, Mathematical modelling of biodegradation in situ application to biodenitrification. *Computers & Mathematics with Applications*, **79** (2020), 1833-1844.
- [2] M. Abaali, J. Harmand and Z. Mghazli, Impact of Dual Substrate Limitation on Biodenitrification Modeling in Porous Media. *Processes*, **8** (2020), 890.
- [3] R.Badge, and N. Adlakha, Finite element model to study potassium dynamics in the rhizosphere of a wheat root due to presence of bio-physical source. *Commun. Math. Biol. Neurosci.* 2019 (2019): Article-ID 8.
- [4] R.Badge, and N. Adlakha, Two-dimensional finite element model to study the effect of water flux on the nitrate dynamics in the rhizosphere of a maize root. *International Journal of Biomathematics* 10.04 (2017), 1750058.
- [5] M. Ballyk and H. Smith, A model of microbial growth in a plug flow reactor with wall attachment. *Mathematical biosciences*, **158** (1999), 95-126.
- [6] M. Ballyk and H. L. Smith, A flow reactor with wall growth. *Mathematical Models in Medical and Health Sciences* (1998).
- [7] D. Bothe, A. Fischer, M. Pierre and G. Rolland, Global wellposedness for a class of reaction-advection-anisotropic-diffusion systems. *Journal of Evolution Equations*, **17** (2017), 101-130.
- [8] F. H. Chapelle, Ground-water microbiology and geochemistry. *John Wiley & Sons* (2000).
- [9] B. E. Christensen and W. G. Characklis, Physical and chemical properties of biofilms. *Biofilms*, **93** (1990), 130.
- [10] B. M. Chen-Charpentier and H. V. Kojouharov, Mathematical modeling of bioremediation of trichloroethylene in aquifers. *Computers & Mathematics with Applications*, **56** (2008), 645-656.
- [11] B. M. Chen-Charpentier, D. T. Dimitrov and H. V. Kojouharov, Numerical simulation

- of multi-species biofilms in porous media for different kinetics. *Mathematics and Computers in Simulation*, **79** (2009), 1846-1861.
- [12] F. Chevron, Dénitrification biologique d'une nappe phréatique polluée par des composés azotés d'origine industrielle: expérimentations en laboratoire sur les cinétiques, le métabolisme et les apports de nutriments (Doctoral dissertation, Lille 1) (1996).
 - [13] J. W. Costerton, Z. Lewandowski, D. E. Caldwell, D. R. Korber and H. M. Lappin-Scott, Microbial biofilms. *Annual review of microbiology*, **49** (1995), 711-745.
 - [14] M. F. Dahab and P. Y. Lee, Nitrate reduction by in-situ bio-denitrification in ground-water. *Water Science and Technology*, **26** (1992), 1493-1502.
 - [15] R. Freter, H. Brickner, J. Fekete, M. M. Vickerman and K. E. Carey, Survival and implantation of *Escherichia coli* in the intestinal tract. *Infection and immunity*, **39** (1983), 686-703.
 - [16] R. Freter, H. Brickner and S. Temme, An understanding of colonization resistance of the mammalian large intestine requires mathematical analysis. *Microecology and Therapy*, **16** (1986), 147-155.
 - [17] J. D. Lambert, Numerical methods for ordinary differential systems: the initial value problem. *John Wiley & Sons, Inc.* (1991).
 - [18] P. L. McCarty, Energetics of organic matter degradation. *Water pollution microbiology* (1972).
 - [19] S. Ouchtout, Z. Mghazli, J. Harmand, J., A. Rapaport and Z. Belhachmi, Analysis of an anaerobic digestion model in landfill with mortality term. *Communications on Pure & Applied Analysis*, **19** (2020), 2333.
 - [20] W. Payne, Reduction of nitrogenous oxides by microorganisms. *Bacteriological reviews*, **37** (1973), 409-452.
 - [21] Z. Xi, J. Guo, J. Lian, H. Li, L. Zhao, X. Liu,.... and J. Yang, Study the catalyzing mechanism of dissolved redox mediators on bio-denitrification by metabolic inhibitors. *Bioresource technology*, **140** (2013), 22-27.